

## Magnetic excitations from the singlet ground state in the $S = \frac{1}{2}$ quasi-one-dimensional system $\text{Sr}_{14-x}\text{Y}_x\text{Cu}_{24}\text{O}_{41}$

M. Matsuda and K. Katsumata

*The Institute of Physical and Chemical Research (RIKEN), Wako, Saitama 351-01, Japan*

H. Eisaki, N. Motoyama, and S. Uchida

*Superconductivity Research Course, University of Tokyo, Bunkyo-ku, Tokyo 113, Japan*

S. M. Shapiro and G. Shirane

*Physics Department, Brookhaven National Laboratory, Upton, New York 11973*

(Received 27 February 1996; revised manuscript received 28 May 1996)

Inelastic neutron scattering measurements have been performed on the  $S = 1/2$  quasi-one-dimensional system  $\text{Sr}_{14-x}\text{Y}_x\text{Cu}_{24}\text{O}_{41}$ , which has both simple chains and two-leg ladders of copper ions. Strong magnetic inelastic peaks, which originate from the simple chains, have been observed at 9–14 meV in  $\text{Sr}_{14}\text{Cu}_{24}\text{O}_{41}$ . These spin gaps have been confirmed to originate from a dimerized state of the chain. The dimers are formed between spins which are separated by 2 and 4 times the distance between the nearest-neighbor copper ions in the simple chain. In addition, a weaker magnetic inelastic peak around 11 meV, which originates from a dimerized state in the ladder, has also been observed. These dimers are formed between the nearest-neighbor copper ions which are connected by the interladder coupling. We have also studied the effect of  $\text{Y}^{3+}$  substitution for  $\text{Sr}^{2+}$  site on the dimerized states. It was found that the yttrium substitution suppresses the gap energies drastically. Possible origins of the dimerized ground state and the excitations are discussed. [S0163-1829(96)05041-2]

### I. INTRODUCTION

A singlet ground state is sometimes realized in interacting magnetic systems because of novel quantum phenomena. One-dimensional (1D) systems with antiferromagnetic interactions are well known to exhibit new types of singlet ground states. For example, in the Haldane system<sup>1</sup> with spin  $S=1$ , the ground state is a singlet which is called the valence-bond-solid (VBS) state.<sup>2</sup> Singlet ground states have also been observed in  $S=1/2$  antiferromagnetically coupled chains (two-leg ladders) such as in  $(\text{VO}_2)\text{P}_2\text{O}_7$  (Ref. 3) and in  $\text{SrCu}_2\text{O}_3$ .<sup>4</sup> The spin-Peierls mechanism also gives a singlet ground state (a dimerized state) in a 1D Heisenberg antiferromagnet, where the driving force is a structural distortion which is caused by the spin-lattice coupling. However, a recent theory<sup>5</sup> discussed the importance of the competing exchange interactions on the spin-Peierls transition found in  $\text{CuGeO}_3$ .<sup>6</sup> Another interesting singlet ground state in an  $S=1/2$  1D magnet was predicted theoretically over 25 years ago by Majumdar and Gosh<sup>7</sup> and later by Haldane.<sup>8</sup> This (dimerized) singlet state is distinguishable from the one found in a spin-Peierls system in that it is not associated with a lattice distortion. The spontaneously dimerized state can be viewed as a superposition of the two states with two neighboring spins: One spin forms a dimer with the spin on its right and the other with the spin on its left.

$\text{Sr}_{14}\text{Cu}_{24}\text{O}_{41}$  is one of the three stable phases of the Sr-Cu-O system which can be synthesized under ambient pressure. The other two stable phases are  $\text{Sr}_2\text{CuO}_3$  which has simple chains of Cu ions and  $\text{SrCuO}_2$  which has zigzag chains of Cu ions. While we attempted to grow a single

crystal of  $\text{SrCuO}_2$ , compound that actually formed was  $\text{Sr}_{14}\text{Cu}_{24}\text{O}_{41}$ . This material itself has a unique structure,<sup>9,10</sup> which contains both simple chains and two-leg ladder chains, and shows interesting magnetic properties. We have already reported the results of magnetic susceptibility and electron spin resonance (ESR) measurements,<sup>11</sup> which show the existence of a dimerized state in this compound. It is interesting to clarify the microscopic nature of the dimerized state by neutron scattering technique.

In this paper, we report the results of inelastic neutron scattering measurements on the  $S=1/2$  quasi-1D system  $\text{Sr}_{14-x}\text{Y}_x\text{Cu}_{24}\text{O}_{41}$ . We have observed strong magnetic inelastic peaks, which originate from the chain, in the energy range 9–14 meV in  $\text{Sr}_{14}\text{Cu}_{24}\text{O}_{41}$ . The gap energies correspond to those estimated from the magnetic susceptibility and ESR measurements.<sup>11</sup> The spin gaps have been confirmed to originate from a dimerized state. The dimers are formed between spins which are separated by 2 and 4 times the distance between the nearest-neighbor copper ions in the chain. In addition, a weaker magnetic inelastic peak around 11 meV, which originates from a dimerized state in the ladder, has also been observed. The dimers are formed between the nearest-neighbor copper ions which are connected by the interladder coupling. We have also studied the effect of  $\text{Y}^{3+}$  substitution for  $\text{Sr}^{2+}$  site on the dimerized states. It has been found that the yttrium substitution suppresses the gap energies drastically.

### II. PRELIMINARY DETAILS

The structure of  $\text{Sr}_{14}\text{Cu}_{24}\text{O}_{41}$  (Refs. 9 and 10) consists of two unique subcells as is shown in Fig. 1(a). One is chains of

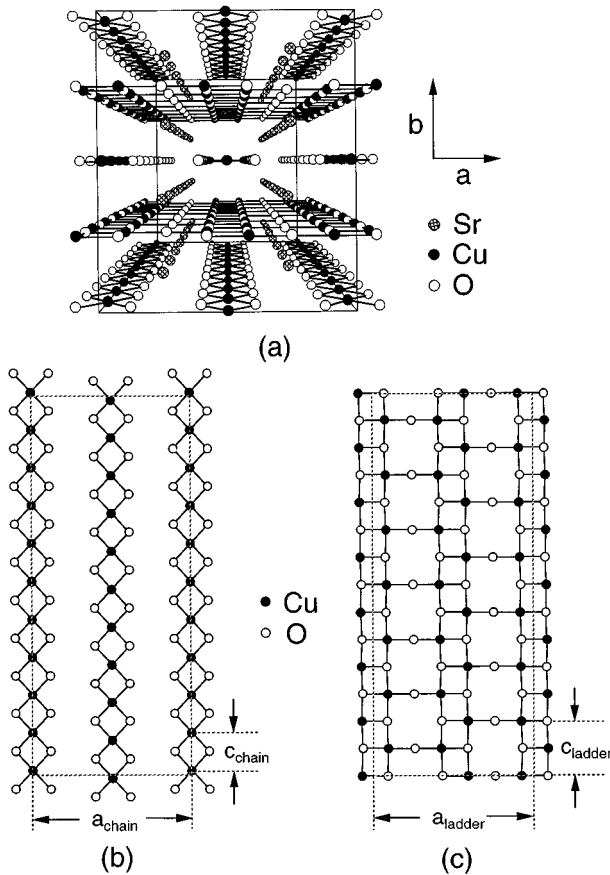


FIG. 1. (a) shows the crystal structure of  $\text{Sr}_{14}\text{Cu}_{24}\text{O}_{41}$  viewed along the  $c$  axis. Solid, open, and shaded circles represent copper, oxygen, and strontium atoms, respectively. (b) and (c) show the chain and the ladder of copper ions in  $\text{Sr}_{14}\text{Cu}_{24}\text{O}_{41}$ , respectively. Solid circles represent copper atoms and open circles oxygen atoms. The dashed rectangles represent the universal unit cell in the (010) crystallographic plane. Here,  $c_{\text{chain}}$  and  $c_{\text{ladder}}$  represent the lattice constant  $c$  for the subcells which contain the chain and the ladder, respectively.

copper ions which are coupled by the nearly  $90^\circ$  Cu-O-Cu bonds shown in Fig. 1(b). The other is two-leg ladders of copper ions, shown in Fig. 1(c), which are coupled by the nearly  $180^\circ$  Cu-O-Cu bonds along the  $a$  and  $c$  axes. Each ladder is coupled by the nearly  $90^\circ$  Cu-O-Cu bonds. The interaction between the ladders is considered to be much weaker than that within the ladder.<sup>12</sup> Each chain and Sr ions form layered structure in the  $ac$  plane and stack alternately along the  $b$  axis. The lattice constants  $a$  and  $b$  are similar in both subcells. On the other hand, the lattice constant  $c$  is much different and has the relation  $10 \times c_{\text{chain}} \approx 7 \times c_{\text{ladder}}$ , where  $c_{\text{chain}}$  and  $c_{\text{ladder}}$  represent the lattice constant  $c$  for the subcell which contains the chain and the ladder, respectively. This means that there are universal large unit cell which contains ten subcells of the chain and seven subcells of the ladder along the  $c$  direction. The space group and the lattice constants of the two subcells and universal cell are<sup>9</sup>

chain subcell:  $Amma$ ,  $a = 11.456 \text{ \AA}$ ,  $b = 13.361 \text{ \AA}$ ,

$$c = 2.749 \text{ \AA};$$

ladder subcell:  $Fmmm$ ,  $a = 11.462 \text{ \AA}$ ,  $b = 13.376 \text{ \AA}$ ,

$$c = 3.931 \text{ \AA};$$

universal cell:  $Pcc2$ ,  $a = 11.459 \text{ \AA}$ ,  $b = 13.368 \text{ \AA}$ ,

$$c = 27.501 \text{ \AA}.$$

We define the Miller index along the  $c$  direction of the chain as  $L_{\text{chain}} = 2\pi/c_{\text{chain}}$  and the ladder as  $L_{\text{ladder}} = 2\pi/c_{\text{ladder}}$ . These are sufficiently different so that by a judicious choice of  $L$ , one can separate the effects of the chain and the ladder.

It is noted that the valence state of copper ions in the stoichiometric  $\text{Sr}_{14}\text{Cu}_{24}\text{O}_{41}$  is +2.25 if one assumes only the valence of Cu changes. It has been reported that there exists excess strontium in  $\text{Sr}_x\text{Cu}_{24}\text{O}_{41}$  ( $x=14.74$ ) (Ref. 9) and oxygen deficiency in  $(\text{Sr}_{0.4}\text{Ca}_{0.6})_{14}\text{Cu}_{24}\text{O}_y$  ( $y=40.07$ ).<sup>13</sup> If these values are taken into account, the valence state of the copper ions becomes +2.11 or the hole concentration is 0.07 per oxygen. The hole carriers are considered to be localized because the compound is highly insulating.<sup>9,14</sup> The trivalent yttrium substitution for divalent strontium is expected to decrease hole carriers. This is consistent with the result of transport measurements which shows that lanthanide doping makes the material more insulating. The lanthanide substitution also affects the crystal structure.<sup>10</sup> Adjacent chains in Y-doped  $\text{Sr}_{14}\text{Cu}_{24}\text{O}_{41}$  are exactly staggered as in  $\text{Sr}_8\text{Ca}_6\text{Cu}_{24}\text{O}_{41}$  structure,<sup>9</sup> whereas the chains of  $\text{Sr}_{14}\text{Cu}_{24}\text{O}_{41}$  are slightly shifted alternately along the  $c$  axis, as shown in Fig. 1(b). The lanthanide substitution also causes small distortion to both the chain and the ladder.

The results of magnetic susceptibility measurements on  $\text{Sr}_{14}\text{Cu}_{24}\text{O}_{41}$  have shown a broad peak below 100 K.<sup>11,13-15</sup> Figure 2 shows the temperature dependence of magnetic susceptibility parallel to the  $c$  axis in a single crystal of  $\text{Sr}_{14}\text{Cu}_{24}\text{O}_{41}$ .<sup>11</sup> The susceptibility decreases with increasing temperature and shows a minimum around 20 K and a broad peak around 80 K. The dashed line in Fig. 2 shows the susceptibility after the Curie-Weiss term, which comes from paramagnetic impurities, was subtracted. The susceptibility becomes almost zero below 20 K. As is discussed by Matsuda and Katsumata,<sup>11</sup> the nearly  $180^\circ$  Cu-O bond length ( $1.90 \text{ \AA}$  perpendicular to the ladder and  $1.97 \text{ \AA}$  along the ladder) of the two-leg ladders in  $\text{Sr}_{14}\text{Cu}_{24}\text{O}_{41}$  is close to the corresponding value in  $\text{SrCu}_2\text{O}_3$  ( $1.93 \text{ \AA}$  perpendicular to the ladder and  $1.97 \text{ \AA}$  along the ladder).<sup>16</sup> Then it is natural

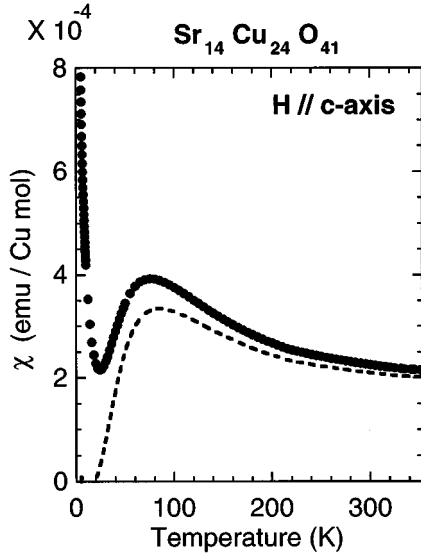


FIG. 2. Temperature dependence of magnetic susceptibility with the external magnetic field parallel to the  $c$  axis in a single crystal of  $\text{Sr}_{14}\text{Cu}_{24}\text{O}_{41}$ . The solid circles represent the observed data. The dotted line represents the susceptibility after the Curie-Weiss term was subtracted.

to assume that the gap energy of the ladder in  $\text{Sr}_{14}\text{Cu}_{24}\text{O}_{41}$  is close to that of  $\text{SrCu}_2\text{O}_3$  (420 K from susceptibility measurements and 680 K from NMR measurements<sup>4</sup>). This means that the ladder in  $\text{Sr}_{14}\text{Cu}_{24}\text{O}_{41}$  has a singlet ground state with a fairly large gap and that the magnetic susceptibility from the ladder is very small below room temperature. Therefore, the susceptibility shown in Fig. 2 suggests that there is a spin gap originating from the chain in this compound.

### III. EXPERIMENTAL METHOD

The single crystals of  $\text{Sr}_{14}\text{Cu}_{24}\text{O}_{41}$  were grown using a traveling solvent floating zone (TSFZ) method at 3 bars oxygen atmosphere. The dimension of the cylindrically shaped crystal used in the experiments is about  $5 \times 5 \times 30 \text{ mm}^3$ . The effective mosaic of the single crystal is less than  $0.4^\circ$  with the spectrometer condition as is described below. The powder samples of  $\text{Sr}_{14-x}\text{Y}_x\text{Cu}_{24}\text{O}_{41}$  ( $x = 0, 1, \text{ and } 3$ ) were prepared by firing stoichiometric ratio of  $\text{SrCO}_3$  (99.99%),  $\text{Y}_2\text{O}_3$  (99.99%), and  $\text{CuO}$  (99.99%) at  $980^\circ\text{C}$  for 30 h in air with intermittent regrinding. Powder x-ray diffraction experiments were performed to check that the reaction was complete. We observed a  $\text{Y}_2\text{Cu}_2\text{O}_5$  phase when  $x$  exceeds 6. We used a similar volume ( $\sim 7 \text{ cm}^3$ ) of the powder samples to perform inelastic neutron measurements. The nuclear Bragg scattering intensities [e.g.,  $(0,4,0)$  and  $(0,0,2)_{\text{ladder}}$ ] from the three different powder samples are similar within an error of 10%. The yttrium doping decreases the lattice constants. Since the structure is layered, it is expected that the substitution will directly affect the distance between the layers along the  $b$  axis with little effect on  $a$ - $c$  plane parameters which are determined by the copper-oxygen connectivity. The lattice constant  $b$  is 13.36 Å and 13.08 Å at 10 K for the  $x=0$  and  $x=3$  samples, respectively. This is consistent with the fact that the ionic radius of  $\text{Y}^{3+}$  is smaller than that of

$\text{Sr}^{2+}$ . This substitution effect on the lattice constants is similar to that in  $(\text{Sr,Ca})_{14}\text{Cu}_{24}\text{O}_{41}$ .<sup>9</sup>

The inelastic neutron scattering experiments were carried out on the H7 and H8 triple-axis spectrometers at the High Flux Beam Reactor at the Brookhaven National Laboratory. For most of the experiments the horizontal collimator sequence was  $40'-40'\text{-S-}40'\text{-}80'$ . The final neutron energy was fixed at  $E_f=14.7 \text{ meV}$ . Pyrolytic graphite single crystals were used as monochromator and analyzer; contamination from the higher-order beam was effectively eliminated using a pyrolytic graphite filter after the sample. The single crystal and powder samples were mounted in closed-cycle refrigerators which allowed us to perform the measurements over a wide temperature range 8–300 K. The experiments for scattering in both the  $(h,0,l)$  and  $(0,k,l)$  zones were performed on the single crystal. From the experiments in these two configurations, we were able to obtain the full information on the energy-versus-momentum ( $\omega$ - $q$  dispersion) relation parallel and perpendicular to the chain and the two-leg ladder direction. As we described in Sec. II, there are three different values for the lattice constant  $c$ . In order to avoid confusion, we will basically use  $c_{\text{ladder}}$  to express Miller indices. Therefore,  $L_{\text{ladder}}=2\pi/c_{\text{ladder}}$  corresponds to the Miller index along the  $c$  axis of the ladder and  $L_{\text{chain}}=2\pi/c_{\text{chain}}=1.42L_{\text{ladder}}$  is the Miller index along the chain.

## IV. MAGNETIC EXCITATIONS

### A. Single crystal of $\text{Sr}_{14}\text{Cu}_{24}\text{O}_{41}$

We show in Fig. 3 inelastic neutron scattering spectra at  $T=8.5 \text{ K}$  at  $(0,0,1)$ ,  $(0,0,1.1)$ , and  $(0,3,-0.25)$  in a single crystal of  $\text{Sr}_{14}\text{Cu}_{24}\text{O}_{41}$ . As discussed below, the measurements near  $(0,0,1)$  correspond to excitations of the ladder and those for small  $L$  ( $L<0.5$ ) are most likely due to the excitations in the chain. The solid lines are the results of fits to a single Gaussian for  $(0,0,1)$  and  $(0,0,1.1)$  and two Gaussians for  $(0,3,-0.25)$ . Two sharp, intense inelastic peaks are observed at  $(0,3,-0.25)$ , whereas a rather weak inelastic peak is observed at  $(0,0,1)$  and  $(0,0,1.1)$ . The linewidth at  $(0,0,1)$  is broader than that at  $(0,0,1.1)$ , where the linewidth is similar to those at  $(0,3,-0.25)$ . This is due to the spectrometer resolution, since one can expect the focusing effect when the resolution ellipsoid is parallel to the dispersion curve. The intrinsic linewidth of the inelastic peaks we observed here is almost resolution limited [calculated energy resolution  $\Delta E=1.7 \text{ meV}$  full width at half maximum (FWHM) at 10 meV]. This focusing effect is the reason we performed the constant- $Q$  scan at  $(0,3,-0.25)$ , not at  $(0,3,0.25)$ .

Figure 4 summarizes the results of the inelastic measurements along the chain and ladder directions in  $\text{Sr}_{14}\text{Cu}_{24}\text{O}_{41}$ . We observe a complicated  $\omega$ - $q$  dispersion relation. The abscissa shows relative values of  $L_{\text{ladder}}$  and  $L_{\text{chain}}$ . Here,  $L_{\text{ladder}}$  represents the Miller indices reciprocal lattice units for the ladder ( $2\pi/c_{\text{ladder}}$ ) and  $L_{\text{chain}}$  for the chain ( $2\pi/c_{\text{chain}}$ ). Excitations are found for  $L_{\text{ladder}}<0.5$  and around  $L_{\text{ladder}}=1$ . As shown in Figs. 3 and 4, the scattered intensities measured for  $L_{\text{ladder}}<0.5$  are greater than that measured near  $L_{\text{ladder}}=1$ . The positions where the dispersion curves show minima correspond to  $L_{\text{chain}}=1/8$  and  $1/4$  and  $L_{\text{ladder}}=1$ . This means that the scattering around  $L_{\text{ladder}}=1$  originates from

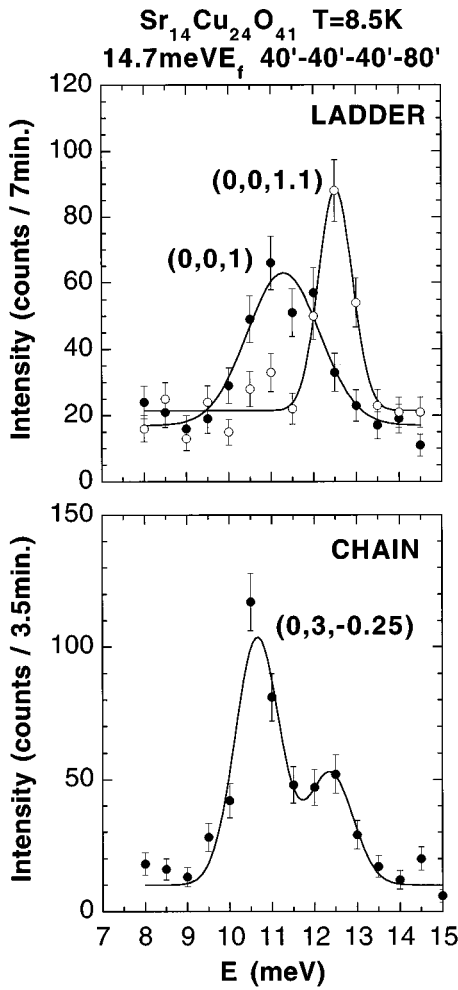


FIG. 3. Inelastic neutron scattering spectra of  $\text{Sr}_{14}\text{Cu}_{24}\text{O}_{41}$  at  $T=8.5\text{ K}$  observed at  $(0,0,1)$ ,  $(0,0,1.1)$ , and  $(0,3,-0.25)$ . The solid lines are the results of fits to single Gaussian for  $(0,0,1)$  and  $(0,0,1.1)$  and two Gaussians for  $(0,3,-0.25)$ .

the ladder. Combining above fact with the gap energies and the dispersion relation along the  $a$  and  $b$  axes as described below, one can conclude that the scattering below  $L_{\text{ladder}}=0.5$  originates from the chain. The intensity of the constant- $Q$  scan integrated over energy are also shown in Fig. 4. The intensity from the chain is about factor of 4 stronger than that from the ladder. The intensity has maximum around  $L_{\text{chain}}=1/4$  and  $L_{\text{ladder}}=1$ . As shown in Fig. 4, the gap energies were observed at 9–13 meV around  $L_{\text{chain}}=1/8$  and  $1/4$  and at 11–14 meV around  $L_{\text{ladder}}=1$ . It is noted that the gap energies observed around  $L_{\text{chain}}=1/8$  and  $1/4$  correspond to the gap energy obtained from the susceptibility ( $\sim 11\text{ meV}$ ) and the ESR measurements ( $\sim 10\text{ meV}$ ),<sup>11</sup> which has been explained as originating from the chain.

One puzzling feature is the presence of two excitations originating from the chain as shown in the spectra of Fig. 3 and the dispersion curve of Fig. 4. The presence of two peaks could be due to the anisotropy in fluctuations parallel and perpendicular to the chain direction or the presence of other interactions. More experimental work is required to clarify their origin.

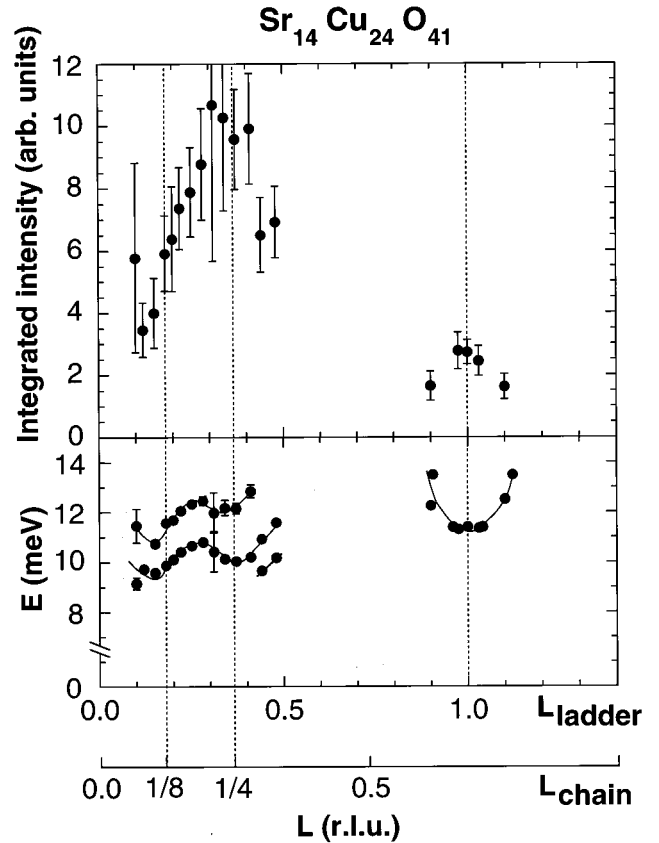


FIG. 4. The dispersion curves and the integrated intensity over energy as a function of  $L$  in  $\text{Sr}_{14}\text{Cu}_{24}\text{O}_{41}$ . Here,  $L_{\text{ladder}}$  represents the reciprocal lattice unit for the ladder and  $L_{\text{chain}}$  for the chain. The solid lines are guides to the eye. The shaded rectangles mean that the peak positions are difficult to be determined in these areas.

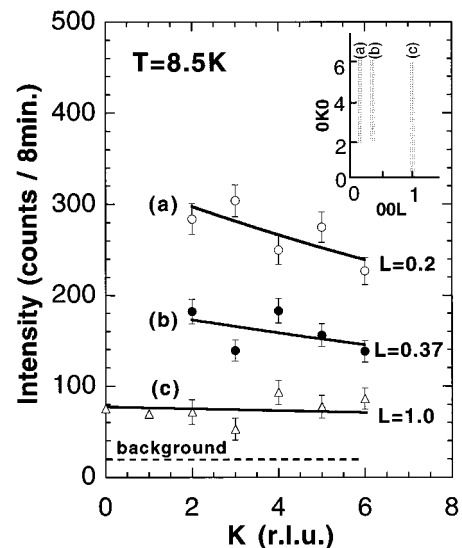


FIG. 5. Peak intensities at  $(0,K,0.2)$ ,  $(0,K,0.37)$ , and  $(0,K,1)$  at  $\Delta E=10, 10,$  and  $11.2\text{ meV}$ , respectively, as a function of  $K$  in  $\text{Sr}_{14}\text{Cu}_{24}\text{O}_{41}$ . The solid lines are guides to the eye. Shaded lines in the inset illustrate the scan trajectories. The background was determined by the intensity on either side of the peaks shown in Fig. 3.

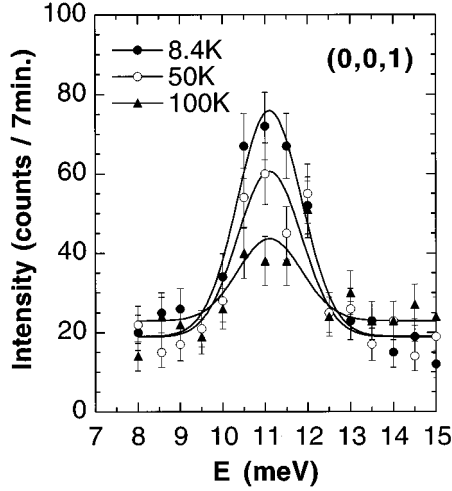


FIG. 6. Temperature dependence of the intensities measured with constant- $Q$  scan at  $(0,0,1)$  in  $\text{Sr}_{14}\text{Cu}_{24}\text{O}_{41}$ . The solid lines are the results of fits to a Gaussian.

Figure 5 shows peak intensities along  $(0,K,0.2)$ ,  $(0, K,0.37)$ , and  $(0,K,1)$  as a function of  $K$ . The intensities gradually decrease as  $K$  is increased. This means that there is little dispersion along the  $b$  direction and that the  $Q$  dependence of the intensities follows the magnetic form factor. We have confirmed that there is no dispersion along the  $a$  and  $b$  axes for the scattering from the chain, and no dispersion along the  $b$  axis and a weak dispersion along the  $a$  axis for the scattering from the ladder. The dispersion curve along  $(H,0,1)$  direction has a maximum around 11 meV at even  $H$  and a minimum around 10 meV at odd  $H$ . These suggest that the scattering from the chain is purely one dimensional and that the scattering from the ladder shows spin correlations along the  $a$  and  $c$  axes. The dispersion relation is consistent with that expected from the structures as shown in Figs. 1(b) and 1(c).

The temperature dependence of the constant- $Q$  scan at the ladder position  $(0,0,1)$  is shown in Fig. 6. The intensity decreases with increasing temperature. The linewidth as well as the gap energy is almost temperature independent. We observed the similar temperature dependence for the constant- $Q$  scans measured at different  $Q$  positions. The peak intensities at  $(1,0,1)$  measured at 9.8 meV and at  $(3,0,0.35)$  at 12.2 meV are plotted against temperature in Fig. 7. The scattering at  $(1,0,1)$  originates from the ladders and the scattering at  $(3,0,0.35)$  from the chains. Both of them have a similar temperature dependence. They are almost constant below  $\sim 20$  K and decrease gradually with increasing temperature. This characteristic temperature dependence identifies the excitations as magnetic and not phonons.

### B. Polycrystalline sample

of  $\text{Sr}_{14-x}\text{Y}_x\text{Cu}_{24}\text{O}_{41}$  ( $x = 0, 1, \text{ and } 3$ )

We show in Fig. 8 inelastic neutron scattering spectra at  $Q=1.12 \text{ \AA}^{-1}$  measured at  $T=10$  K in the powder samples of  $\text{Sr}_{14-x}\text{Y}_x\text{Cu}_{24}\text{O}_{41}$  ( $x=0, 1, \text{ and } 3$ ). It is noted that the magnetic contribution comes only from the chain at  $Q=1.12 \text{ \AA}^{-1}$ , which corresponds to  $0.7c^*$ . This is schematically illustrated in the inset of Fig. 9. A flat-topped inelastic peak is

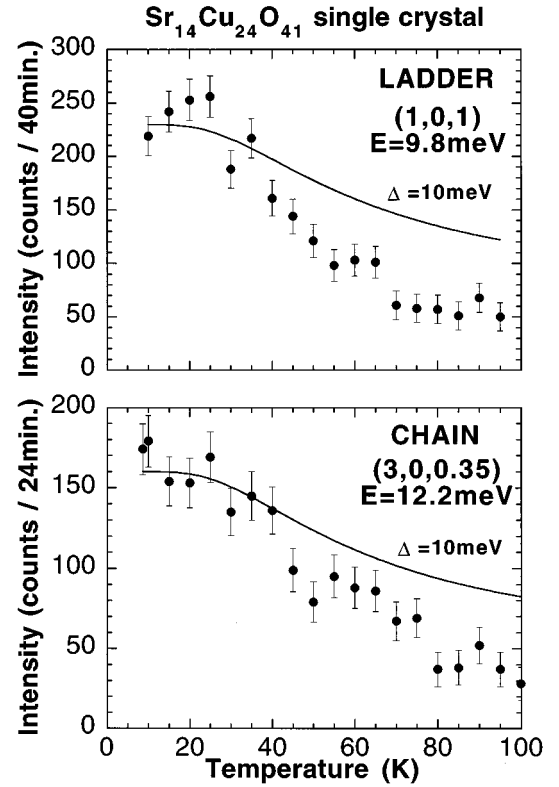


FIG. 7. Temperature dependence of the peak intensities at  $(1,0,1)$  measured with 9.8 meV and at  $(3,0,0.35)$  with 12.2 meV in  $\text{Sr}_{14}\text{Cu}_{24}\text{O}_{41}$ . The solid lines are the results of fits to Eq. (2) with  $\Delta=10$  meV.

observed between 10 and 14 meV in the  $x=0$  sample. This is consistent with the  $\omega$ - $q$  dispersion relation of the single crystal as shown in Fig. 4.

The constant- $\omega$  scan with  $\omega=11$  meV at  $T=10$  K in  $\text{Sr}_{14}\text{Cu}_{24}\text{O}_{41}$  powder sample is shown in Fig. 9. The intensity decreases gradually with increasing  $Q$ . It is expected that there is a peak in intensity at the  $Q$  position which corresponds to the distance between the coupled moments. We could not reach this  $Q$  position because momentum and energy conservation cannot be satisfied at low  $Q$  at energy transfer of 11 meV with the spectrometer configuration described in Sec. III. As shown in the inset of Fig. 9, the contribution from the ladder is superposed above  $Q=1.6 \text{ \AA}^{-1}$ , which corresponds to  $1c^*$ . However, we did not observe anomaly around  $Q=1.6 \text{ \AA}^{-1}$ . This is because the scattering from the ladder is rather small compared to that from the chain and the spectrometer resolution function may broaden the small anomaly. The  $Q$  dependence of the magnetic scattering intensity in an  $S=1/2$  noninteracting dimer system<sup>17</sup> is given by

$$I(Q) \propto F^2(Q) \left( 1 - \frac{\sin QR}{QR} \right), \quad (1)$$

where  $F(Q)$  is the magnetic form factor of  $\text{Cu}^{2+}$  and  $R$  is the separation between the spins which form the dimers. The dashed and dotted lines in Fig. 9 show the calculated values from Eq. (1) with  $R=4c_{\text{chain}}$  and  $c_{\text{ladder}}$ , respectively. We fixed the ratio of the intensity from the chain ( $I_{\text{chain}}$ ) to that

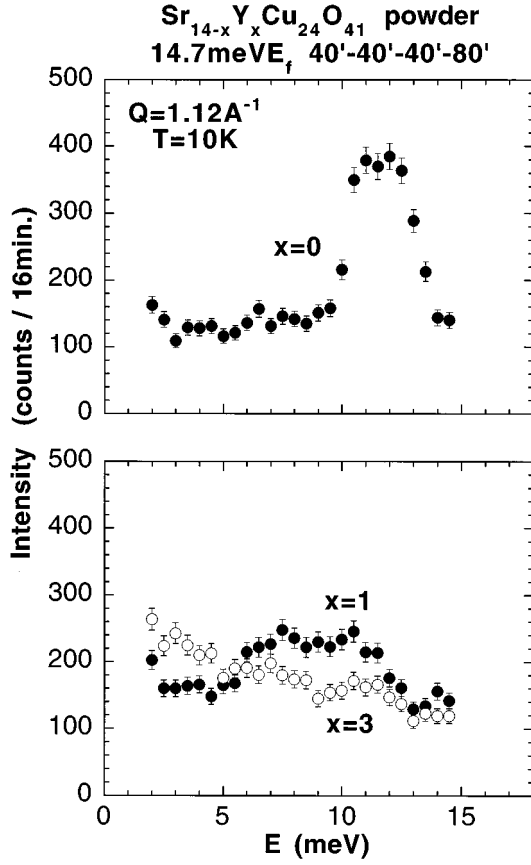


FIG. 8. The constant- $Q$  scans at  $Q=1.12 \text{ \AA}^{-1}$  measured at  $T=10 \text{ K}$  in the powder samples of  $\text{Sr}_{14-x}\text{Y}_x\text{Cu}_{24}\text{O}_{41}$  ( $x=0, 1,$  and  $3$ ).

from the ladder ( $I_{\text{ladder}}$ ) as  $I_{\text{chain}}/I_{\text{ladder}}=4$ , which is the case in the single-crystal experiments as mentioned above. The solid line represents the sum of the two lines and the background. This simple approximation seems to reproduce the experimental results rather well. In fact, this data yielded us valuable information as to the presence of excitations from the chains.

When the yttrium is substituted in the strontium site, the gap energies are suppressed. The  $x=1$  sample shows a broader flat-topped peak between 6 and 13 meV and the peak intensity becomes about half of the  $x=0$  sample as shown in Fig. 8. The integrated intensity is almost the same as the  $x=0$  sample. The  $x=3$  sample does not show any peaks but a tail which decreases with increasing energy.

## V. DISCUSSION

We have observed that spin gaps exist both in the chain and the ladder. As shown in Fig. 7, the inelastic scatterings from both the chain and the ladder have similar temperature dependence which may be explained by the model based on noninteracting dimers. In an  $S=1/2$  noninteracting dimer system which has a nonmagnetic singlet ground state with  $S=0$  and a triplet excited state with  $S=1$ , when the intradimer coupling is antiferromagnetic, the energy-loss part of the neutron cross section ( $\sigma$ ) is proportional to the population of the ground state:

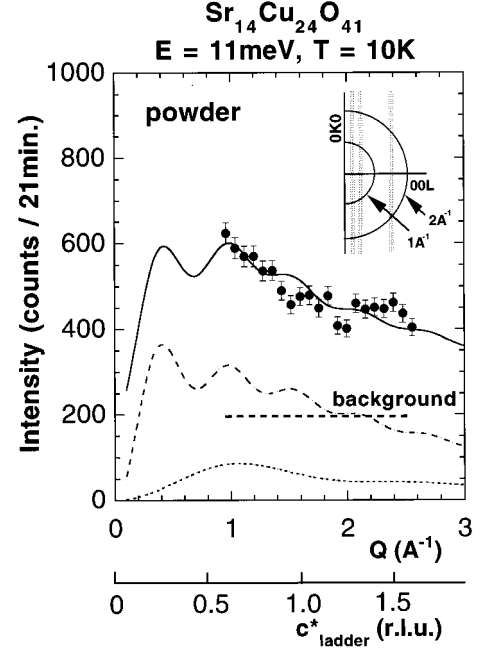


FIG. 9. The constant- $\omega$  scan with  $\omega=11 \text{ meV}$  at  $T=10 \text{ K}$  in  $\text{Sr}_{14}\text{Cu}_{24}\text{O}_{41}$  powder sample. The inset shows the scattering configurations in the  $(100)$  crystallographic plane. The shaded lines represent the 1D magnetic Bragg planes. The solid half-circles represent assemblies of the scattering vectors with  $Q=1 \text{ \AA}^{-1}$  and  $2 \text{ \AA}^{-1}$ . The dashed and dotted lines represent the calculated values from Eq. (1) with  $R=4c_{\text{chain}}$  and  $c_{\text{ladder}}$ , respectively. The solid line represents the sum of the two lines and the background.

$$\sigma(\omega) \propto \frac{1}{1 + 3 \exp(-\Delta/k_B T)} \delta(\hbar\omega - \Delta), \quad (2)$$

where  $\Delta$  is the energy gap between the ground and excited states and  $k_B$  is Boltzmann's constant. The solid lines in Fig. 7 show the calculated values from Eq. (2) with  $\Delta=10 \text{ meV}$ . This simple approximation reproduces the experimental results at low temperatures. However, the observed values decrease more rapidly with increasing temperature than Eq. (2) predicts, which suggests the contribution from more complex states as shown in Fig. 4. The dispersion along the  $c$  axis shows the correlation between the dimers.

We now discuss the origin of the dimerized state observed in  $\text{Sr}_{14}\text{Cu}_{24}\text{O}_{41}$ . First, we discuss the dimerized state in the chain. We have found from the present study that the magnetic excitations have long-range correlations, 2 and 4 times the distance between  $\text{Cu}^{2+}$  spins. As mentioned in Sec. II, in order to fulfill the requirement for stoichiometry, either some of the Cu ions should be trivalent or holes are created at the oxygen sites. It is believed that creating a  $\text{Cu}^{3+}$  in oxides costs larger energy than putting a hole into oxygen. A bond-valence-sum calculation has shown that  $\text{Cu}^{3+}$  ions (in other words, holes) preferably exist in the chain.<sup>18</sup> One can estimate that the number of holes in the chain is 27% of the Cu ions in the chain in  $\text{Sr}_{14.74}\text{Cu}_{24}\text{O}_{40.07}$  and 60% in  $\text{Sr}_{14}\text{Cu}_{24}\text{O}_{41}$ . Since  $\text{Sr}_{14}\text{Cu}_{24}\text{O}_{41}$  is highly insulating, the holes are considered to be localized at oxygen sites. However, hopping of these holes from one oxygen site to the other is possible. This hopping mechanism will make the

exchange interactions between  $\text{Cu}^{2+}$  spins longer ranged. It is noted that Curie-type susceptibility at low temperatures should increase considerably if the isolated  $\text{Cu}^{2+}$  ions are produced. However, the magnetic impurity density, calculated from the Curie constant assuming  $\text{Cu}^{2+}$  as impurities, is estimated to be only  $\sim 1.4\%$ .<sup>11</sup> Therefore, it is expected that most of the  $\text{Cu}^{2+}$  ions in the chain form dimers.

If we have two neighboring  $\text{Cu}^{2+}$  spins coupled antiferromagnetically to form a singlet, we expect to see a gap at  $L_{\text{chain}}=1/2$ . However, the observed  $\omega$ - $q$  dispersion curve shows a minimum at  $L_{\text{chain}}=1/4$  where the intensity is also a maximum. This difference suggests that there is an additional doubling along the chain direction. One possible explanation for this would be the one based on the competing nearest-neighbor ( $J_1$ ) and next-nearest-neighbor ( $J_2$ ) interactions model. The Hamiltonian describing the system is expressed as

$$H = J_1 \sum_{i=1}^{N-1} \vec{S}_i \cdot \vec{S}_{i+1} + J_2 \sum_{i=1}^{N-2} \vec{S}_i \cdot \vec{S}_{i+2}. \quad (3)$$

As discussed by Tonegawa and Harada<sup>19</sup> and by Zeng and Parkinson,<sup>20</sup> the phase modulation of the spin-spin correlation functions follows a pattern  $(- + - + \dots)$  for  $J_2/J_1 \leq 0.5$  and  $(- - + + - - + + \dots)$  for  $J_2/J_1 \geq 0.5$ . In the latter case, they showed a broad maximum in the Fourier transform of the spin correlation function ( $S(Q)$ ) at  $L_{\text{chain}}=1/4$ . Then one can expect a minimum of the  $\omega$ - $q$  dispersion curve at  $L_{\text{chain}}=1/4$ . Further-neighbor interactions and/or many spin correlations will realize a pattern  $(- - - - + + + + - - - - + + + + \dots)$  and give a minimum of the  $\omega$ - $q$  dispersion curve at  $L_{\text{chain}}=1/8$ . Another possibility to explain the magnetic excitations with longer-ranged correlations is the following. We consider the case where the holes with  $S=1/2$  are coupled with  $\text{Cu}^{2+}$  with  $S=1/2$  next to them and form a nonmagnetic state. Then the dimers can be formed between spins which are separated by 2 and 4 times the distance between the nearest-neighbor copper ions in the chain. In this case, the  $\omega$ - $q$  dispersion relation will show minima at the positions which correspond to  $L_{\text{chain}}=1/8$  and  $1/4$ . A puzzle remaining in the two cases mentioned above is why we do not see additional scattering from the chains at higher-order positions such as  $L_{\text{chain}}=3/4$ .

Next, we discuss the dimerized state in the ladder. As described in Sec. II, it is expected that the spin gap energy which originates from the intraladder coupling is above 35 meV. In this case, because of the antiferromagnetic coupling the dispersion curve is expected to have minima at  $(0,0, L_{\text{ladder}})$  when  $L_{\text{ladder}}=(n+1)/2$  or at  $(H_{\text{ladder}}, 0, 0)$  when  $H_{\text{ladder}}=(n+1)/2$  ( $n$  an integer). The former corresponds to the dimers which are formed along the  $c$  axis and the latter along the  $a$  axis. However, we have observed minima of the dispersion at  $(0,0, L_{\text{ladder}})$  where  $L_{\text{ladder}}=2n+1$  ( $n$  an integer) or at  $(H_{\text{ladder}}, 0, 0)$  where  $H_{\text{ladder}}=2n+1$  ( $n$  an integer). Therefore, the dimerized states, which we observed in the ladder, are formed between the nearest-neighbor copper ions which are connected by the interladder coupling. Since the intensity is much weaker than that from the chain, the dimers

are considered to be dilute. If we assume that there are no holes and that all the copper sites have spins, the concentration of the copper spins which contribute to the interladder dimers in the ladders becomes  $\sim 25\%$  from an estimation using the integrated intensity shown in Fig. 4. This concentration is the upper limit. The interladder dimers may be formed between spins which cannot form the intraladder dimer. The interladder coupling constant is estimated to be antiferromagnetic and have a value of  $\sim 11$  meV, which is similar to that in  $\text{CuGeO}_3$ .<sup>6</sup> This means that the ratio between the interladder ( $\sim 11$  meV) and the intraladder ( $\sim 100$  meV) interactions is  $\sim 0.1$ . This probably applies to the coupling constants in  $\text{SrCu}_2\text{O}_3$ .<sup>4,16</sup>

We showed that  $\text{Y}^{3+}$  substitution for  $\text{Sr}^{2+}$  decreases the spin gap energies. It is noted that the substitution effect on the chain is clear but that on the ladder is difficult to define because the contribution from the ladder is small in  $\text{Sr}_{14}\text{Cu}_{24}\text{O}_{41}$ . If the decrease of the lattice constants with the substitution affects the dimerized states, the superexchange interaction between  $\text{Cu}^{2+}$  spins becomes stronger and so the gap energy increases. This suggests that the decrease of the holes and/or the structural distortion mainly affect the dimerized states. The number of holes in the chain is 50% of that of Cu ions in the chain of  $\text{Sr}_{13}\text{Y}_1\text{Cu}_{24}\text{O}_{41}$  and 30% in  $\text{Sr}_{11}\text{Y}_3\text{Cu}_{24}\text{O}_{41}$ . This drastic change of hole number will largely change the electronic states of Cu and oxygen. The decrease of hole number probably makes the exchange interaction between  $\text{Cu}^{2+}$  spins shorter ranged and the dimerized state becomes unstable. Then the chains in  $\text{Sr}_{14-x}\text{Y}_x\text{Cu}_{24}\text{O}_{41}$  behave like an  $S=1/2$  1D Heisenberg antiferromagnet which has no gap in the excitation spectra.<sup>21</sup>

In conclusion, we have performed inelastic neutron scattering measurements on the  $S=1/2$  quasi-1D system  $\text{Sr}_{14-x}\text{Y}_x\text{Cu}_{24}\text{O}_{41}$ , which has both chains and two-leg ladders of copper ions. Strong magnetic inelastic peaks, which originate from the chain, have been observed at 9–14 meV in  $\text{Sr}_{14}\text{Cu}_{24}\text{O}_{41}$ . The spin gaps have been confirmed to originate from a dimerized state. The dimers are formed between spins which are separated by 2 and 4 times the distance between the nearest-neighbor copper ions in the chain. In addition, a weaker magnetic inelastic peak around 11 meV, which originates from a dimerized state in the ladder, has also been observed. The dimers are formed between the nearest-neighbor copper ions which are connected by the interladder chain coupling. We have also studied the effect of  $\text{Y}^{3+}$  substitution for  $\text{Sr}^{2+}$  site on the dimerized states. It has been found that the yttrium substitution suppresses the gap energies drastically. Possible origins of the dimerized ground state and the excitations are discussed.

## ACKNOWLEDGMENTS

We would like to thank G. Castilla, V. J. Emery, M. Hase, S. A. Kivelson, G. Tataru, and A. Zheludev for many helpful discussions. This work was partially supported by the U.S.-Japan Cooperative Program on Neutron Scattering operated by the U.S. Department of Energy and the Japanese Ministry of Education, Science, Sports and Culture, by the NEDO International Joint Research Grant, and by a Grant from the

Yazaki Memorial Foundation for Science and Technology. Work at Brookhaven National Laboratory was carried out under Contract No. DE-AC02-76CH00016, Division of Material Science, U.S. Department of Energy. The work at the

Institute of Physics and Chemical Research (RIKEN) was partially supported by a Grant-in-Aid for Scientific Research from the Japanese Ministry of Education, Science, Sports and Culture.

- 
- <sup>1</sup>F. D. M. Haldane, *Phys. Rev. Lett.* **50**, 1153 (1983).  
<sup>2</sup>I. Affleck, T. Kennedy, E. H. Lieb, and H. Tasaki, *Phys. Rev. Lett.* **59**, 799 (1987).  
<sup>3</sup>D. C. Johnston, J. W. Johnson, D. P. Goshorn, and A. J. Jacobson, *Phys. Rev. B* **35**, 219 (1987).  
<sup>4</sup>M. Azuma, Z. Hiroi, M. Takano, K. Ishida, and Y. Kitaoka, *Phys. Rev. Lett.* **73**, 3463 (1994).  
<sup>5</sup>G. Castilla, S. Chakravarty, and V. J. Emery, *Phys. Rev. Lett.* **75**, 1823 (1995).  
<sup>6</sup>M. Hase, I. Terasaki, and K. Uchinokura, *Phys. Rev. Lett.* **70**, 3651 (1993).  
<sup>7</sup>C. K. Majumdar and D. K. Gosh, *J. Math. Phys.* **10**, 1399 (1969).  
<sup>8</sup>F. D. M. Haldane, *Phys. Rev. B* **25**, 4925 (1982).  
<sup>9</sup>E. M. McCarron, III, M. A. Subramanian, J. C. Calabrese, and R. L. Harlow, *Mater. Res. Bull.* **23**, 1355 (1988).  
<sup>10</sup>T. Siegrist, L. F. Schneemeyer, S. A. Sunshine, J. V. Waszczak, and R. S. Roth, *Mater. Res. Bull.* **23**, 1429 (1988).  
<sup>11</sup>M. Matsuda and K. Katsumata, *Phys. Rev. B* **53**, 12 201 (1996).  
<sup>12</sup>T. M. Rice, S. Gopalan, and M. Sigrist, *Europhys. Lett.* **23**, 445 (1993).  
<sup>13</sup>M. Uehara, M. Ogawa, and J. Akimitsu, *Physica C* **255**, 193 (1995).  
<sup>14</sup>M. W. McElfresh, J. M. D. Coey, P. Strobel, and S. von Molnar, *Phys. Rev. B* **40**, 825 (1989).  
<sup>15</sup>M. Kato, H. Chizawa, Y. Koike, T. Noji, and Y. Saito, *Physica C* **235-240**, 1327 (1994).  
<sup>16</sup>Z. Hiroi, M. Azuma, M. Takano, and Y. Bando, *J. Solid State Chem.* **95**, 230 (1991).  
<sup>17</sup>H. Güdel, A. Stebler, and A. Furrer, *Inorg. Chem.* **18**, 1021 (1979).  
<sup>18</sup>M. Kato, K. Shiota, and Y. Koike, *Physica C* **258**, 284 (1996).  
<sup>19</sup>T. Tonegawa and I. Harada, *J. Phys. Soc. Jpn.* **56**, 230 (1987).  
<sup>20</sup>C. Zeng and J. B. Parkinson, *Phys. Rev. B* **51**, 11 609 (1995).  
<sup>21</sup>J. des Cloizeaux and J. J. Pearson, *Phys. Rev.* **128**, 2131 (1962).